Scientific Journal for Damietta Faculty of Science **14**(3) 2024, 76-89
doi: 10.21608/sjdfs.2025.327142.1185
ISSN Print 2314-8594
ISSN Online 2314-8616

https://sjdfs.journals.ekb.eg/

Histological and Histochemical Investigations on the Toxic Effects of Acrylamide and Ameliorative Effects Using Moringa oleifera Leave Nanoparticles on the Liver, Kidney, and Testis of Adult Male Rats

Kadry El-Bakry[1], Nahed Omar[1], Lamiaa Deef[1], Shereen Fahmy[1] and Abdullah Yaquob[1]

[1]Zoology Department, Faculty of Science, Damietta University, Damietta, Egypt.

Received: 10 October 2024 /Accepted: 17 October 2024

*Corresponding author's E-mail: yacoopa@students.du.edu.eg

Abstract

The present study was conducted to evaluate the toxic effects resulted from acrylamide (ACR) and the protective effects of *Moringa oleifera* (*M. oleifera*) nanoparticles to adult male rats. Twenty adult male rats were randomly divided into four groups: Group I (Control group); Group II (Acrylamide group): rat received 50 mg/kg b.wt. of ACR in drinking water for 3 weeks; Group III (*M. oleifera* nanoparticles group): rats received 50 mg/kg b.wt of *M. oleifera* nanoparticles daily for 3 weeks; and Group IV (*M. oleifera* nanoparticles + Acrylamide group): rats were given 50 mg/kg b.wt of ACR and received *M. oleifera* nanoparticles 50 mg/kg b.wt orally, daily, at the same time for 3 weeks. Blood and tissue samples were collected for physiological histological, and histochemical studies.

The histological study revealed that rats exposed to ACR had significant damage to their kidneys, livers, and testicles, along with inflammatory changes and structural deformities. Treatment with *M. oleifera* nanoparticles improve histopathological changes and reduced susceptibility to ACR toxicity in adult male rats. Three-week treatment of *M. oleifera* nanoparticles largely recovers the reduction in proteins and carbohydrates observed in ACR administration. The application of *M. oleifera* nanoparticles with ACR significantly reduces the histochemical damage that is caused by ACR. The treatment also reduces ACR's destructive impact on activities of ALT, AST enzymes, and MDA, creatinine, and urea levels while increasing SOD enzyme activity. From the results one can suggest that *M. oleifera* nanoparticles are a potential cytoprotective agent against ACR's pathological toxicity.

Keywords: ACR, M.oleifera, Physiology, Histology, Histochemistry.

Introduction

Acrylamide (ACR) is mostly found in food items made from low-protein, high-carb raw materials that have been heat-treated to temperatures exceeding 120°C. ACR has been shown to be genotoxic, neurotoxic, and reproductively harmful to animals. As such,

ACR could be neurotoxic to people **(Ahn *et al*., 2002; Jamshidi and Zahedi, 2015).** According to many research, individuals typically consume 0.3–0.6 g/kg of body weight of ACR every day. Children and teenagers are more sensitive than other age groups because they often consume more foods such chips, crackers, and french fries that contain added sugar (ACR) **(Kadawathagedara *et al*., 2018).** Compared to other tissues, blood exhibits the highest concentration of accumulation after ingestion, inhalation, or intradermal exposure to ACR **(Shipp *et al*., 2006)**. One of the primary negative effects of ACR is oxidative stress, which is believed to be the root of the liver's recurrent injury. Lipid peroxidase activity is increased, and antioxidant defense systems are lowered when reactive oxygen species are produced, resulting in oxidative damage **(Dobrzynska *et al*., 2004).**

Additionally, research has shown that glycidamide might be produced from ACR via the cytochrome P450 route. The signal pathway and cellular activity may then change as a result, creating a DNA-reactive epoxide **(Tornqvist, 2005).** ACR has a high water solubility, which allows it to diffuse and distribute quickly throughout the body's organs, including the liver and kidney. Furthermore, ACR accumulates in these organs and may be harmful because of its ability to form adducts with hemoglobin **(Belhadj *et al*., 2019).** Previous studies have examined the detrimental effects of ACR on the liver and kidney tissues in animal models **(Rizk *et al*., 2018).** The rats exposed to ACR had statistically significant increases in their levels of ALT and AST as well as increased lipid peroxidation as compared to the rats in the control and treatment groups **(Al Syaad *et al*., 2023).** Rats given ACR for liver slices had dilated central veins, nuclear degeneration in hepatocytes, and pyknotic Von Kupffer cells in the hepatic sinusoids. There was dilatation of the portal vein, bile duct, and hepatic artery. When compared to the control group, the ACR group's mean AST and ALT enzyme values were significantly higher. Malondialdehyde (MDA) and superoxide dismutase (SOD) levels in the liver homogenate were significantly higher in the ACR group than in the control group **(El-Sharouny *et al*., 2016).** The kidney group with ACR had high blood flow in the interstitial vessels and severe hydropic degeneration and coagulation necrosis in the tubular epithelium. A statistically significant ($p < 0.05$) difference was found when comparing the experimental group to the control group. Serum creatinine and urea concentrations increased significantly ($p < 0.05$) after ten days of oral therapy with ACR in comparison to the control group **(Kandemir *et al*., 2020).** ACR is a biologically hazardous substance that interacts with enzymes involved in DNA replication, resulting in cell mutations and DNA damage that causes local tumors during the early stages of carcinogenesis **(Klaunig, 2008).**

Another study found that eliminating free radicals with natural dietary antioxidants produces cells that are resistant to oxidative damage. Moringa oleifera (*M. oleifera*) is a member of the Brassica order and belongs to the Moringaceae family, which is made up of a single genus with around thirteen species **(Mahmood *et al*., 2010).** *M. oleifera* is a native Indian medicinal plant that has become more well-known in tropical and subtropical areas **(Fahey, 2005).** Numerous studies have shown the effectiveness of *M. oleifera* leaves and seed extract as antioxidants that protect against the damaging effects of oxidative stress and free radical attack, according to **Prakash *et al*. (2007)**. Moreover, *M. oleifera* contains significant concentrations of a variety of essential phytochemicals (enzymes), including catalase, polyphenol oxidase, ascorbic acid oxidase, total phenols, and vitamins **(Aboulthana *et al*., 2021a).** Remarkably, studies have shown that the antioxidant activity of M. oleifera leaf extract which has a high concentration of phytoconstituents may be enhanced by the addition of silver nanoparticles (Ag-NPs) **(Aboulthana *et al*., 2021b).** *M. oleifera* leaves exhibit important DNA protection qualities, according to **Sikder *et al*. (2013)** research, indicating that they may be consumed by humans to prevent oxidative DNA damage and cell damage. Ag-NP's applications are widely acknowledged in a broad range of sectors, including chemistry, medicine, electronics, and catalysis. Ag-NPs may be made in a variety of methods. Because biological methods of producing Ag-NPs employ non-toxic substances, they are seen as environmentally beneficial. Precisely reducing and stabilizing the nanoparticles are the actions of flavonoids, terpenes, proteins, enzymes, lipids, antioxidants, glycoproteins, and tannins **(Ramaswamy *et al*., 2019).** In the present study, adult male rats were used to assess the

protective effects of *M. oleifera* nanoparticles against ACR and its detrimental effects.

Materials and Methods

Preparation of Moringa oleifera Extract.

Ten grams of powder and one hundred milliliters of distilled water are combined to create the *M. oleifera* extract. This was mixed to dissolve the powder, and then heated for 10 minutes, or until the extracted solution took on a light green hue. Filter paper was used to filter the extract, which was then stored at 4 °C to preserve it for use as *M. oleifera* extract later **(Nilanjuna *et al*., 2014 and Abdel-Rahman *et al*., 2022)**.

Synthesis of Silver Nanoparticles (Ag-NPs) Carried by Moringa oleifera

In the experiment, 190 mL of a 2 mM silver nitrate solution and 10 mL of *M. oleifera* extract were combined while being continuously stirred. The solution becomes dark brown after being stirred in a magnetic stirrer for four hours at room temperature and then let to sit in the dark for twenty-four hours. Following a minimum of 20 minutes of centrifugation at 5000 rpm at a constant temperature, the solution was allowed to condense into pellets. After discarding the supernatant, the granules were dispersed in distilled water once again and let to air dry before being preserved for further use **(Nilanjuna *et al*., 2014 and Abdel-Rahman *et al*., 2022)**.

Characterization of silver nanoparticles derived from M. oleifera

According to our recently published study **(Abduljalil *et al*., 2023 and Abduljalil *et al*., 2024)**, *M. oleifera* silver nanoparticles were produced and characterized using an advanced confirmatory process (Transmission Electronic Microscopy and Dynamic Light Scattering (DLS) and Zeta Potential), and an ultraviolet-visible spectrophotometer (UV-VIS).

Experimental Design

The rats were weighed at around 150 grams each and were randomly divided into four groups of equal numbers (five rats per group) as follows:

1- **Group I (Control group):** rats received nothing additional to their normal diet.
2- **Group II (Acrylamide group):** rats were given 50 mg/kg body weight of ACR in their drinking water daily for three weeks **(LoPachin *et al*., 2006 and Gawesh *et al*., 2021).**
3- **Group III (*M. oleifera* nanoparticles group):** rats received 50 mg/kg body weight of *M. oleifera* nanoparticles orally daily for three weeks **(Malathi *et al*., 2018 and Ramaswamy *et al*., 2019).**
4- **Group IV (*M. oleifera* nanoparticles + Acrylamide group):** Rats were given 50 mg/kg body weight of ACR and received *M. oleifera* nanoparticles at 50 mg/kg body weight simultaneously orally, daily, for three weeks **(Malathi *et al*., 2018 and Ramaswamy *et al*., 2019).**

Ethical statement

The study's experimental methods and the care of the animals followed Dammitta University's (Egypt) ethical standards for research. DuRec no. 33 is the study's ethical approval code.

Collection of blood samples

Rats were anesthetized using chloroform. Then, all blood samples were extracted from the heart using 5 mL syringes. The blood samples were put into sterile tubes with ethylenediamine tetraacetic acid (EDTA) as an anticoagulant to assess the activity of the kidney and liver enzymes determinations.

Tissue samples collection

After blood samples collected, the liver, kidney and testis tissues were taken out and preserved in 10% formalin before being processed normally and embedded in paraffin. Slices 5 µm thick were cut and stained with hematoxylin and eosin (H&E) dye for microscopic examination **(Drury *et al*., 1976)**. The dye slices were examined under a light

microscope and captured on camera. Histochemical analysis reveals total proteins (bromophenol blue) **(Mazia *et al.*, 1953),** and polysaccharides **(**periodic acid schiff's reaction**,** PAS reaction) (**Pearse, 1985).**

Statistical Analysis

Version 25 of the SPSS software was used to conduct statistical analysis. Every result was evaluated using one-way variance analysis tests (ANOVA). Statistical significance was defined as $p<0.05$, and the results were expressed as mean (M) ± standard deviation (SD) (N=5).

Results

Physiological study

Alanine / Aspartate aminotransferase enzyme activities (ALT/AST)

According to the present study's results, the mean activities of ALT and AST enzymes in the ACR group compared to the control group increased statistically significantly after three weeks of oral administration of ACR at a dosage of 50 mg/kg b.wt. **(Table 1)**. After administering *M. oleifera* nanoparticles to the rats for three weeks at a dosage of 50 mg/kg b.wt., the mean ALT and AST activity in the *M. oleifera* nanoparticles and *M. oleifera* nanoparticles + ACR groups were decreased significantly than those in the ACR group. One-way ANOVA statistical analysis revealed that all groups had an extremely significant difference in the mean values of ALT and AST ($p< 0.000$). In fact, statistical analysis shows that rats that were given both *M. oleifera* nanoparticles and *M. oleifera* nanoparticles + ACR at the same time had lower mean ALT and AST activities than rats that were only given ACR ($p< 0.000$). Moreover, there was a significant difference in the AST mean activity between the *M. oleifera* silver nanoparticle-treated rats and the control group ($p< 0.000$). However, there was no significant difference in the ALT mean value between the *M. oleifera* nanoparticle-treated rats and the control group ($p> 0.05$).

Creatinine and Urea levels

The current study's findings indicate that after three weeks of oral administration of ACR at a dose of 50 mg/kg b.wt., the mean levels of creatinine and urea in the ACR group compared to the control group increased statistically significantly **(Table 1)**. The mean creatinine and urea levels in the *M. oleifera* nanoparticles and *M. oleifera* nanoparticles + ACR groups were considerably lower than those in the ACR group during the three weeks of administration of *M. oleifera* nanoparticles to the rats at a dose of 50 mg/kg b.wt. The creatinine and urea levels in each group differed significantly ($p<0.000$), according to a one-way ANOVA statistical analysis. According to statistical analysis, rats that received *M. oleifera* nanoparticles and *M. oleifera* nanoparticles + ACR at the same time had lower mean creatinine and urea levels than rats that received ACR alone ($p<0.000$). Additionally, there was a significant difference ($p<0.000$) in the mean levels of creatinine and urea between the rats treated with *M. oleifera* silver nanoparticles and the control group.

Table 1: The mean activities of ALT/AST enzymes and the mean levels of creatinine and urea in different experimental groups.

Enzymes	Group I	Group II	Group III	Group IV	P value
	Mean ± SD	Mean ± SD	Mean ± SD	Mean ± SD	
ALT (U/L)	42.80±3.49 [a]	76.80±5.76 [b]	49.60±3.04 [a]	55.20±5.44 [c]	0.000*
AST (U/L)	196.20±2.38[a]	258.60±2.07[b]	213.40±2.07[c]	226.80±1.92 [d]	0.000*
Creatinine (mg/dl)	0.68±0.08 [a]	2.28±0.26 [b]	1.04±0.15 [c]	1.54±0.05 [d]	0.000*
Urea (mg/dl)	37.20±2.20 [a]	55.40±2.07 [b]	44.80±2.86 [c]	48.20±2.04 [d]	0.000*

The data is presented as Mean ± SD (N = 5 for each group).(*) Extremely significant, $p\leq 0.000$ versus those of the control group. a, b, c, and d mean having different superscript letters in the same column differ significantly ($p< 0.05$). Group I: Control group; Group II: Acrylamide group; Group III: *M. oleifera* nanoparticles group; and the : Group IV *M. oleifera* nanoparticles + Acrylamide group.

Superoxide dismutase (SOD U/ml) and Malondialdehyde (MDA nmol/ml) enzyme activities

The current study's findings indicate that after three weeks of oral administration of ACR at a dose of 50 mg/kg b.wt., the mean levels of MDA in the ACR group compared to the control group increased statistically considerably, which correlated with a

significant decrease in SOD **(Table 2)**. The mean MDA values in the *M. oleifera* nanoparticles and *M. oleifera* nanoparticles + ACR groups significantly decreased after giving M. *oleifera* nanoparticles to the rats for three weeks at a dosage of 50 mg/kg b.wt. The SOD mean activity significantly increased when compared to the ACR group. The statistical analysis using one-way ANOVA showed that there was a very significant difference ($p<0.000$) in the mean activities of SOD and MDA across all groups. Rats that received *M. oleifera* nanoparticles and *M. oleifera* nanoparticles + ACR together really had greater mean SOD value and lower mean MDA than rats that received ACR alone ($p<0.000$), according to statistical analysis. Furthermore, the MDA mean value differed significantly ($p>0.05$) between the rats treated with *M. oleifera* nanoparticles and the control group. Nonetheless, there was no statistically significant difference in the mean SOD value between the rats treated with *M. oleifera* nanoparticles and the control group ($p<0.000$).

Table 2: The mean activities of SOD / MDA enzymes in different experimental groups.

Enzymes	Group I	Group II	Group III	Group IV	P value
	Mean ± SD	Mean ± SD	Mean ± SD	Mean ± SD	
SOD (U/ml)	207.17±2.11[a]	181.10±3.16[b]	204.11±3.46 [a]	197.12±2.24 [c]	0.000*
MDA (nmol/ml)	10.28±0.17 [a]	20.36±1.10 [b]	12.96±0.85 [c]	15.81±0.83 [d]	0.000*

The data is presented as Mean ± SD (N = 5 for each group).(*) Extremely significant, p≤ 0.000 versus those of the control group. a, b, c, and d mean having different superscript letters in the same column differ significantly ($p< 0.05$). Group I: Control group; Group II: Acrylamide group; Group III: *M. oleifera* nanoparticles group; and the Group IV: *M. oleifera* nanoparticles + Acrylamide group.

Histological study (Hematoxylin and Eosin stains).

A- (Liver tissue).

The hepatic tissue structure in the livers of control rats was normal, with no evident pathological alterations. Hepatocytes organize into cords from the central veins to the portal regions, with sinusoids separating them. Hepatocytes display central vesicular nuclei with eosinophilic cytoplasm. Binucleated nuclei are found in certain cells. The blood sinusoids contain kupffer cells **(Fig. 1 A).** Administration of ACR caused the central vein to congest, some hepatocytes to necrotize, the cytoplasm to vacuolated, the hepatocytes to lose their cellular borders, more kupffer cells to activate, and an invasion of inflammatory cells **(Fig. 1 B).** Nanoparticles from the *M. oleifera* group demonstrated the proper structure of the liver lobule. Hepatocyte cords surround the lobule's central vein. Hepatocytes contain strongly eosinophilic granulated cytoplasm and spherical nuclei. Hepatic sinusoids are frequently detected in the spaces between the strands of hepatocytes **(Fig. 1 C).** The nanoparticles from *M. oleifera* have greatly reduced the harmful effects of ACR on this group, as shown by the vacuolated cytoplasm. Adding nanoparticles from *M. oleifera* to rats that had been given ACR made the liver tissues' structure much better, as shown by the normal periportal hepatic cells that were found in the liver after staining it with hematoxylin and eosin **(Fig. 1 D).**

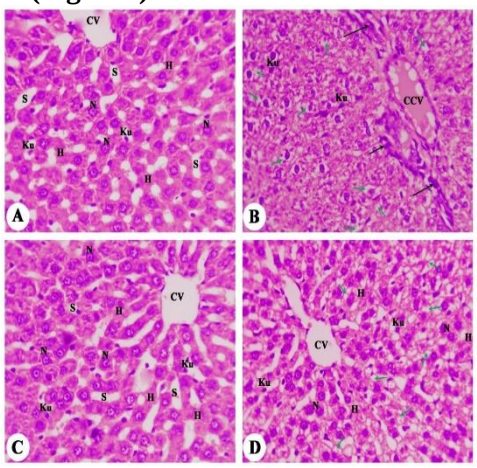

Figure (1): A) A photomicrograph of the rat liver of the Group I (Control group) showing normal hepatic architecture. CV: central vein, H: hepatocyte, N: nucleus, Ku: kupffer cell and S: sinusoid. **B)** A photomicrograph of the rat liver of the Group II (Acrylamide group) showing abnormal hepatic architecture. CCV: congested central vein, Ku: kupffer cells, green arrow: vacuolated cytoplasm and Black arrow: inflammatory cells infiltration. **C)** A photomicrograph of the rat liver from the Group III (*M. oleifera* nanoparticles group) showing normal hepatic architecture .CV: central vein, H: hepatocyte, N: nucleus, Ku: kupffer cells and S: sinusoid. **D)** A photomicrograph of the rat liver from the Group IV (*M. oleifera* nanoparticles + Acrylamide group) showing a nearly normal hepatic architecture. CV: central vein, H: hepatocyte, Ku: kupffer cell and green arrow: vacuolated cytoplasm. H&E X400.

B-(Kidney tissue).

Rats in control exhibited normal renal tissue structure and no overt pathological alterations in kidney tissue sections. Normal renal tubules and glomeruli with Bowman's capsule were seen **(Fig. 2 A).** The kidneys of rats that had been injured by ACR showed glomeruli atrophy with widening of Bowman's space, degeneration and necrosis of the epithelium of the renal tubules, and infiltration and bleeding of inflammatory cells into the renal interstitial space **(Fig. 2 B).** The treated nanoparticles from the *M. oleifera* group showed normal renal architecture in a portion of the kidney. Nanoparticles from the *M. oleifera* group demonstrated normal renal corpuscle architecture and renal tubule appearance. The renal glomeruli and tubules exhibit normal histology **(Fig. 2 C).** In rats that had received ACR administration, supplementation with *M. oleifera* nanoparticles for three weeks significantly improved the structure of the kidney tissues. Hematoxylin and eosin staining of the renal tubular epithelium in the kidney revealed a decrease in the level of moderate degenerative changes **(Fig. 2 D).**

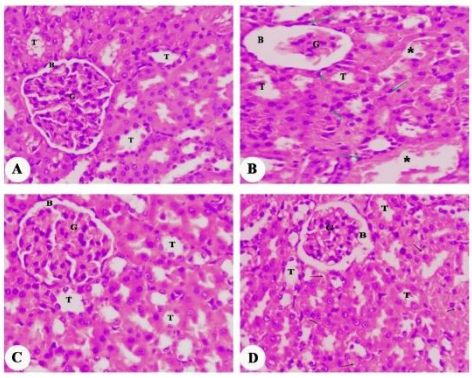

Figure (2): A) A photomicrograph of the rat kidney of the Group I (Control group) shows preserved kidney architecture. G: glomerulus, B: Bowman's capsule; T: renal tubule. **B)** A photomicrograph of rat kidneys in the Group II (Acrylamide group) showing the G: glomerulus, B: Bowman's capsule, T: renal tubule, green arrow: inflammatory infiltration, and *: necrosis. **C)** A photomicrograph of the rat kidney from the Group III (*M. oleifera* nanoparticles group) showing the G: glomerulus, B: Bowman's capsule, and T: renal tubules. **D)** A photomicrograph of the rat kidney from the Group IV (*M. oleifera* nanoparticles + Acrylamide group) showing the G: glomerulus, B: Bowman's capsule, T: renal tubules, black arrow: vacculation. H&E X400.

C- (Testis tissue).

Testis sections from control rats showed normal seminiferous tubules, represented by the presence of all germinal cells. Control rat testes stained with hematoxylin and eosin show spermatogenic cells and seminiferous tubules that are normal and arranged in a straight line **(Fig. 3 A).** The ACR administration leads to the appearance of abnormal signs such as depletion of germinal cells, formation of giant cells, and widening of the interstitial spaces between seminiferous tubules **(Fig. 3 B).** The nanoparticles of the *M. oleifera* group did not include any histological testicular lesions. The healthy part of this group's testes had all the spermatogenic series, mature active seminiferous tubules, and normal histological structure **(Fig. 3 C).** After administering ACR and *M. oleifera* nanoparticles to rats simultaneously for three weeks, they dramatically enhanced spermatogenesis, with the exception of certain germinal cells, which had some histological abnormalities related to ACR **(Fig. 3 D).**

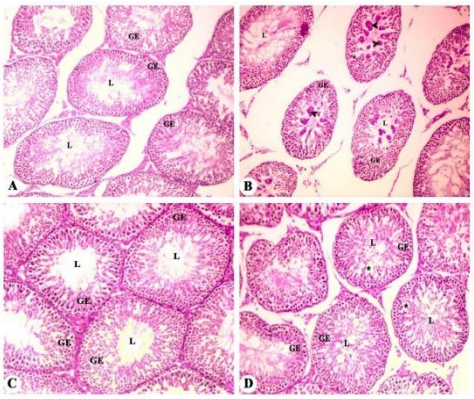

Figure (3): A) A photomicrograph of the rat testis of the Group I (Control group) showing normal testicular morphology. GE: germinal epithelium and L: lumen. **B)** A photomicrograph of the rat testis of the Group II (Acrylamide group) showing the GE: germinal epithelium, L: lumen, *: germinal cell depletion and head arrow: giant cell formation. **C)** A photomicrograph of the rat testis from the Group III (*M. oleifera* nanoparticles group) showing the normal structure of the testis. GE: germinal epithelium and L: lumen. **D)** A photomicrograph of the rat testis from the Group IV (*M. oleifera* nanoparticles + Acrylamide group) showing the GE: germinal epithelium, L: lumen and *: degeneration of germinal cell epithelium. H&E X400.

Histochemical study for carbohydrates (PAS stain).

A-(Liver tissue).

Hepatocyte cytoplasm, as well as the connective tissue surrounding the central vein in the liver of control rats, had a strong positive response to PAS. Evident are kupffer cells. The liver cells also demonstrated the commonly observed phenomenon of glycogen flight **(Fig. 4 A).** Rats that were given ACR for three weeks had a lot fewer hepatocytes and PAS-positive materials that were spread out unevenly, showing up as random patches. Meanwhile, a large number of vacuoles inside the hepatocytes were seen **(Fig. 4 B).** The hepatocytes of rats treated with *M. oleifera* nanoparticles had almost normal PAS positive reactivity **(Fig. 4 C).** ACR administration, followed by supplementation with M. oleifera nanoparticles for three weeks, caused a small drop in the PAS positive reactivity of the rats' hepatocytes compared to the control group. However, rats exposed to ACR + *M. oleifera* nanoparticles for three weeks showed the very same PAS reactivity in their liver cells as the control group **(Fig. 4 D).**

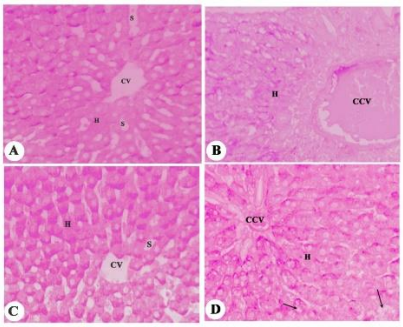

Figure (4): A) Photomicrograph of male rat liver section of the Group I (Control group) showing uniform distribution of PAS +ve reaction in the cytoplasm of hepatocytes surrounding CV. CV: central vein, S: sinusoid and H: hepatocyte **B)** Photomicrograph of male rat liver section of the Group II (Acrylamide group) showing diminished PAS +ve reaction in the cytoplasm of hepatocytes surrounding CV. CCV: congested central vein and H: hepatocyte **C)** Photomicrograph of male rat liver section of the Group III (*M. oleifera* nanoparticles group) showing uniform distribution of PAS +ve reaction in the cytoplasm of hepatocytes surrounding CV. CV: central vein, S: sinusoid and H: hepatocyte **D)** Photomicrograph of male rat liver section of the Group IV (*M. oleifera* nanoparticles + Acrylamide group) showing moderate PAS +ve reaction around the CV. CCV: congested central vein, H: hepatocyte and black arrow: vacuolated cytoplasm. PAS 400X.

B-(Kidney tissue).

A strong PAS response was seen in the kidneys of the control rats in the glomeruli and brush borders of the uriniferous tubules **(Fig. 5 A).** Following three weeks of ACR therapy, there was a significant reduction in PAS positive material with obvious cellular damage **(Fig. 5 B).** Rat kidneys treated with *M. oleifera* nanoparticles showed a strong PAS reaction in the glomeruli and brush borders of the uriniferous tubules **(Fig. 5 C).** However, giving rats ACR and then supplementing with *M. oleifera* nanoparticles for three weeks caused a small drop in the PAS positive reactivity in the glomeruli and uniniferous tubules **(Fig. 5 D).**

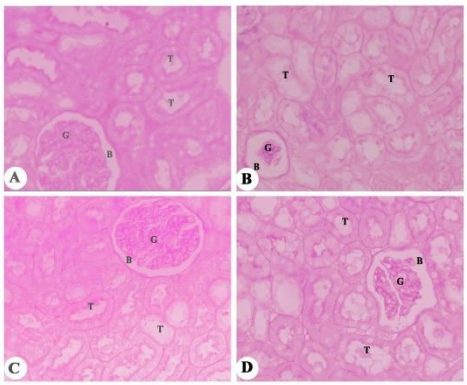

Figure (5): A) Photomicrograph of male rat kidney section of the Group I (Control group) showing uniform distribution of PAS +ve reaction in the renal architecture. G: glomeruli, B: Bowman's space and T: Renal tubules **B)** Photomicrograph of male rat kidney sections of the Group II (Acrylamide group) showing diminished PAS +ve reaction in the renal architecture. G: glomeruli, B: Bowman's space and T: Renal tubules **C)** Photomicrograph of male rat kidney section from the Group III (*M. oleifera* nanoparticles group) showing uniform distribution of PAS +ve reaction in the renal architecture. G: glomeruli, B: Bowman's space and T: Renal tubules **D)** Photomicrograph of male rat kidney section of the Group IV (*M. oleifera* nanoparticles + Acrylamide group) showing moderate distribution of PAS +ve reaction in the renal architecture. G: glomeruli, B: Bowman's space and T: Renal tubules. PAS 400X**.**

C-(Testis tissue).

The testes of control rats showed significant PAS reactivity, particularly in the spermatozoa, border membranes, and interstitial cells **(Fig. 6 A).** The rats' testes after three weeks of ACR administration showed a significant loss of PAS-positive material, as

well as a noticeable deterioration of the seminiferous tubules and spermatozoa **(Fig. 6 B).** The testes of rats treated with *M. oleifera* nanoparticles had almost normal PAS positive reactivity. The boundary membranes around the seminiferous tubules continued to be highly stained in the meantime **(Fig. 6 C).** The testis of the rats given ACR plus *M. oleifera* nanoparticle supplementation for three weeks showed a slight decrease in PAS positive reactivity when compared to the control group. On the other hand, after three weeks of exposure to ACR + *M. oleifera* nanoparticles, rats' seminiferous tubules and spermatozoa clearly recovered and restored PAS-positive materials **(Fig. 6 D).**

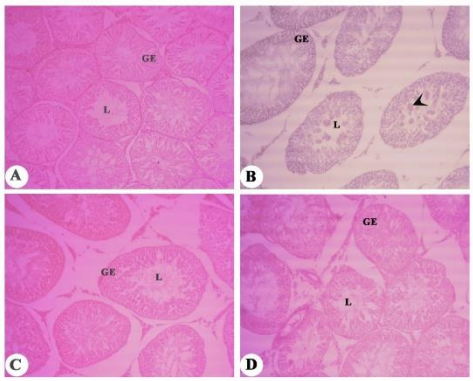

Figure (6): A) Photomicrograph of rat testis section of the Group I (Control group) showing uniform distribution of PAS +ve reaction in the testicular architecture. GE: germinal epithelium and L: lumen. **B)** photomicrograph of the rat testis of the Group II (Acrylamide group) showing diminished PAS +ve reaction in the testicular architecture. GE: germinal epithelium, L: lumen and head arrow: giant cell formation. **C)** Photomicrograph of rat testis section from the Group III (*M. oleifera* nanoparticles group) showing uniform distribution of PAS +ve reaction in the testicular architecture. GE: germinal epithelium and L: lumen. **D)** Photomicrograph of rat testis section from the Group IV (*M. oleifera* nanoparticles + Acrylamide group) showing moderate distribution of PAS +ve reaction in the testicular architecture**.** GE: germinal epithelium and L: lumen. PAS 400X.

Histochemical study for total protein (Bromophenol Blue stain).

A-(Liver tissue).

The liver of control rats exhibited strong responses to bromophenol blue in both the hepatocytes and the connective tissue around the central veins **(Fig.7 A).** Hepatocytes from rats administered ACR for three weeks showed a significant loss of lymphocytes around the central veins as well as an uneven distribution of materials labeled with protein inside the liver cells. The hepatocytes had many vacuoles and cell injuries **(Fig. 7 B).** The hepatocytes of rats treated with *M. oleifera* nanoparticles had almost normal bromophenol blue positive reactivity **(Fig. 7 C).** Administration of ACR and then supplementation with *M. oleifera* nanoparticles for three weeks showed a significant recovery of protein-stained materials. The architecture of the hepatic tissue seemed normal **(Fig. 7 D).**

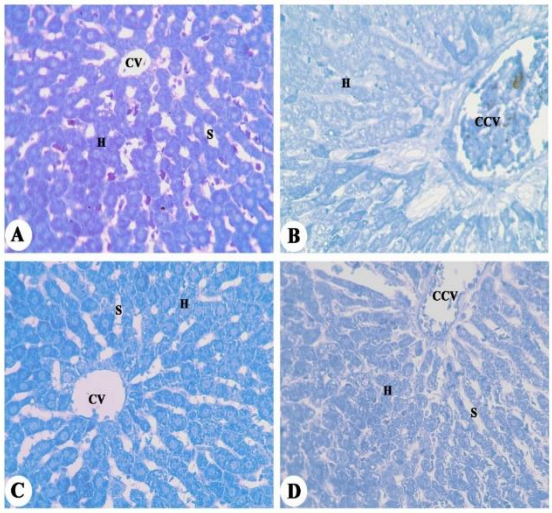

Figure (7): A) Photomicrograph of male rat liver section of the Group I (Control group) showing uniform distribution of PAS +ve reaction in the cytoplasm of hepatocytes surrounding CV. CV: central vein, S: sinusoid and H: hepatocyte **B)** Photomicrograph of male rat liver section of the Group II (Acrylamide group) showing diminished PAS +ve reaction in the cytoplasm of hepatocytes surrounding CV. CCV: congested central vein and H: hepatocyte **C)** Photomicrograph of male rat liver section of the Group III (*M. oleifera* nanoparticles group) showing uniform distribution of PAS +ve reaction in the cytoplasm of hepatocytes surrounding CV. CV: central vein, S: sinusoid and H: hepatocyte **D)** Photomicrograph of male rat liver section of the Group IV (*M. oleifera* nanoparticles + Acrylamide group) showing moderate PAS +ve reaction around the CV. CCV: congested central vein, H: hepatocyte and S: sinusoid. PAS 400X.

B-(Kidney tissue).

The kidneys of control rats had a strong reaction to bromophenol blue in the glomeruli, collecting tubules, and uriniferous cysts **(Fig. 8 A).** The glomeruli, unriniferous, and collecting

tubules showed a significant reduction in protein-stained material after given ACR for three weeks. The glomeruli, uriniferous, and collecting tubules' protein-stained materials decreased as a result of administering ACR; in the meanwhile **(Fig. 8 B).** Rat kidneys treated with *M. oleifera* nanoparticles showed a strong reaction to bromophenol blue in the glomeruli, uriniferous and collecting tubules **(Fig. 8 C).** The kidneys of the rats given ACR plus *M. oleifera* nanoparticle supplementation for three weeks demonstrated a notable recovery and restoration of protein-stained materials in the glomeruli, uriniferous, and collecting tubules **(Fig. 8 D).**

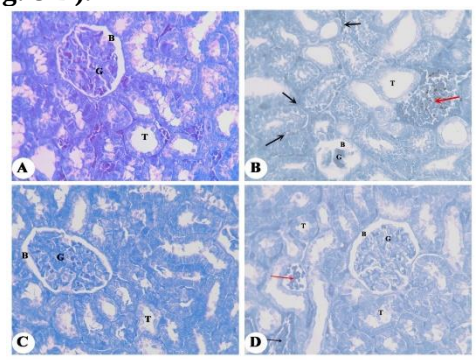

Figure (8): A) Photomicrograph of male rat kidney section of the Group I (Control group) showing uniform distribution of PAS +ve reaction in the renal architecture. G: glomeruli, B: Bowman's space and T: Renal tubules **B)** Photomicrograph of male rat kidney sections of the Group II (Acrylamide group) showing diminished PAS +ve reaction in the renal architecture. G: glomeruli, B: Bowman's space, T: Renal tubules, Red arrow: Interstitial hemorrhage and Black arrow: Interstitial inflammatory infiltration **C)** Photomicrograph of male rat kidney section from the Group III (*M. oleifera* nanoparticles group) showing uniform distribution of PAS +ve reaction in the renal architecture. G: glomeruli, B: Bowman's space and T: Renal tubules **D)** Photomicrograph of male rat kidney section of the Group IV (*M. oleifera* nanoparticles + Acrylamide group) showing moderate distribution of PAS +ve reaction in the renal architecture. G: glomeruli, B: Bowman's space, T: Renal tubules, Red arrow: Interstitial hemorrhage and Black arrow: Interstitial inflammatory infiltration**.** PAS 400X**.**

C-(Testis tissue).

The tests of control rats exhibited a strong response to total proteins in the spermatogenic cells, the interstitial cells, and the border membranes enclosing the seminiferous tubules **(Fig. 9A).** The testes of the rats that were given ACR for three weeks showed a clear loss of protein in the spermatogenic cells, interstitial cells, and border membranes around the seminiferous tubules **(Fig. 9 B).** The testes of rats treated with *M. oleifera* nanoparticles had almost normal bromophenol blue reactivity. The boundary membranes around the seminiferous tubules continued to be highly stained in the meantime **(Fig. 9 C).** After three weeks of given ACR plus *M. oleifera* nanoparticle supplementation, the rats' testicles demonstrated a significant recovery of protein-stained material in most spermatogenic phases **(Fig. 9 D).**

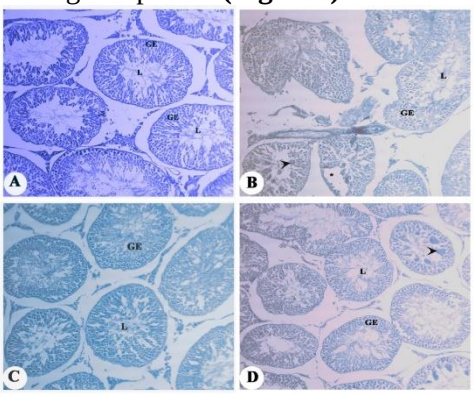

Figure (9): A) Photomicrograph of rat testis section of the Group I (Control group) showing uniform distribution of PAS +ve reaction in the testicular architecture.GE: germinal epithelium and L: lumen. **B)** photomicrograph of the rat testis of the Group II (Acrylamide group) showing diminished PAS +ve reaction in the testicular architecture. GE: germinal epithelium, L: lumen and head arrow: giant cell formation. **C)** Photomicrograph of rat testis section from the Group III (*M. oleifera* nanoparticles group) showing uniform distribution of PAS +ve reaction in the testicular architecture. GE: germinal epithelium and L: lumen. **D)** Photomicrograph of rat testis section from the Group IV (*M. oleifera* nanoparticles + Acrylamide group) showing moderate distribution of PAS +ve reaction in the testicular architecture**.** GE: germinal epithelium, L: lumen and head arrow: giant cell formation. PAS 400X.

Discussion

The purpose of this study was to assess the simultaneous effects of treating adult male rats with acrylamide (ACR) and *M. oleifera* nanoparticles. The study's histology results showed that rats given ACR had notable damage to their livers, kidneys, and testicles, as well as severe inflammatory changes and

structural deformities in these organs. The treatment of ACR results in a number of adverse effects, including vacuolated cytoplasm, hepatocyte apoptosis, cellular loss, increased activity of kupffer cells, and movement of inflammatory cells. The results of **El-Sharouny *et al*. (2016)**, which showed cytoplasmic enlargement, nuclear degeneration, and dilated central veins in liver sections, are consistent with this. According to **Mahmood *et al*. (2015)**, rats administered ACR showed liver degeneration, blocked blood vessels, and inflammatory cell infiltration; in contrast, high-dose mice had considerable infiltration and blocked blood vessels. These findings are consistent with the current investigation. According to studies, ACR may lead to hepatotoxicity by inducing changes in liver histology, increasing oxidative stress, and changing the function of biomarker enzymes (ALT and AST). Hepatocellular membrane damage is often indicated by elevated serum aminotransferase activity, especially ALT **(Gowda *et al*., 2009 and Rizk *et al*., 2018).**

M. oleifera nanoparticles may reduce histological changes caused by ACR in rats by reducing epithelial hypertrophy, preventing blood clot formation in sinusoids, and maintaining normal periportal hepatocytes in the liver segment. This is in line with the results of El-bakry et al. (2016), who found that *M. oleifera* extract enhances inflammation-related cell infiltration, hepato-fatty degeneration, and liver structural disruption. Furthermore, **Dharmendra et al. (2014)** found that a stable blood total bilirubin level after injection of *M. oleifera* extract indicates better hepatocyte cell activity. The findings emphasize the possible health hazards connected to exposure to ACR. In rats, nanoparticles from *M. oleifera* showed anti-hepatotoxic effects, reducing ALT and AST levels, suggesting early cell membrane integrity improvement. According to the present study, a findings comparable to that of **Omeodu and Uahomo (2023)**, diabetic rats given mixed leaf extract from *M. oleifera* exhibited decreased ALT and AST activity compared to rats that did not receive any therapy. The present study corroborates the findings of **Aboulthana *et al*. (2021b)**, which demonstrated that the nano-extract significantly reduced enzyme biomarkers in both therapy modalities and restored normal levels when compared to samples induced by colon cancer. This suggests that the extract protects the structural integrity of the hepatocyte membrane against reactive oxygen species. Furthermore, Moringa seed extract may stop liver MDA levels from increasing and SOD activity from decreasing, according to a research by **Hamza, 2010** . This suggests that the antioxidants in the extract may guard against the toxicity and fibrosis caused by carbon tetrachloride.

The histological analysis of the kidneys showed bleeding, glomeruli atrophy, tubule epithelium degeneration, and inflammatory cell infiltration. These findings corroborated those of **Sun *et al*. (2020)**, who reported kidney fragmentation, glomerular congestion, hemorrhage, tubular necrosis, cell swelling, and mononuclear cell infiltration in addition to glomerular congestion. Moreover, **Kandemir *et al*. (2020)** discovered that severe hydropic degeneration and marked hyperemia in the interstitial vessels of kidneys with ACR were caused by coagulation necrosis in the tubular epithelium. According to the findings, giving rats *M. oleifera* nanoparticles prevented renal alterations brought on by ACR and restored normal kidney architecture. This is in line with the results of **Akinrinde *et al*. (2020)**, which demonstrated enhanced renal histology, reduced glomerular lesions, decreased inflammation, and enhanced indices of the endothelium, glomerular, tubular, and interstitial scoring systems. Additionally, the extract demonstrated the potential to preserve tissue, maintaining glomeruli and guaranteeing urine excretion. In fact, **Saleh (2018)** research discovered that rats administered *M. oleifera* extract had kidney architecture and collagen fiber distribution that was almost normal, with no breakdown of the tubule epithelial cell lining.

The testicular histological study revealed abnormalities in the testis and epididymis, including reduced germinal cells, giant cell growth, and increased interstitial gaps between seminiferous tubules. These findings align with **Bhuiyan *et al.* (2023)** findings that rats with ACR showed altered testis and epididymis due to spermatogenesis cessation. Also, **Fiedan *et al*. (2015)** found that ACR-treated testis showed degeneration of spermatogenic cells and formatin within seminiferous tubules after two weeks, with spermatogonia and sertoli cells appearing after three weeks due to severe degeneration and extensive coagulative necrosis. The study found that *M. oleifera* nanoparticles reduced ACR-induced changes in

rats' testicles and restored their structure, indicating spermatogenesis restoration. This aligns with **Alkafafy *et al.* (2021)** findings, which showed normal seminiferous tubules, spermatogenic cell layers, and more free spermatozoa in the lumen of the *M. oleifera* extract group. In addition, **Kamalrudin *et al*. (2018)** found that the testicular tissue of the *M. oleifera*-treated group showed no microscopic damage or disorganization, with spermatozoa packed in the lumen.

It was clear from the PAS reaction findings that ACR had harmful effects on the metabolism of carbohydrates. The rats received ACR therapy for 11 days at a dosage of 50 mg/kg body weight, a metabolic disease that affects energy metabolism pathways and interferes with ACR may be the cause of weight loss **(Ghorbel *et al.*, 2017).** The results of this study suggest that liver damage from ACR may have caused the decreased amount of carbohydrates in the liver. In addition, the histological analysis of the liver tissue showed adverse alterations, including hepatocytes with localized necrosis. The present research revealed that rats given ACR had altered livers, exhibiting hydropic vacuolated degenerations in the cytoplasm and pycnotic nuclei. Additionally, exposure to ACR resulted in dilated and congested blood sinusoids and the central vein, as well as the infiltration of inflammatory cells. **(Al Syaad *et al.*, 2023).** According to **Karimi *et al*. (2020)**, liver slices from the ACR group showed pyknosis, lipid deposits, infiltration of inflammatory cells, and congestion of red blood cells. According to this study, the renal damage that occurred as a consequence of ACR may have contributed to the reduced quantity of carbohydrates in the kidneys. The kidney's histological examination revealed changes caused by ACR, including renal glomeruli atrophy, necrosis, tubular necrosis, glomeruli hypertrophy, hemorrhage, and edema around the blood vessels **(Al Syaad *et al.*, 2023).** According to **Ozbek (2012)**, oxidative stress, its associated mediators, and inflammation play a major role in the pathogenesis of a number of renal diseases and their consequences. Renal lipid composition has a high content of long-chain polyunsaturated fatty acids, which may contribute to the kidney's high susceptibility to injury from reactive oxygen species. Oxidative stress has gained significant traction in molecular mechanism research for renal disorders. The histopathological feature may result from the build-up of free radicals in the renal tissue of rats injected with ACR, which is caused by elevated levels of MDA and H_2O_2 products **(Ghorbel *et al.*, 2017).** Similarly, spermatogenic cell loss and lipid peroxidation may be responsible for the testicular depletion of carbohydrate resources. In comparison to the control group, the histological data revealed many histopathological changes in the ACR group. Among the anomalies that were seen were edema, degenerative vacuolar changes, and protein material infiltration between tubules. Along with distortion and tortuosity of the basement membrane, the seminal tubule tissue displayed sperm cell changes, sloughing off, and desquamation of spermatogenic cells **(Al Syaad *et al*., 2023).**.

In the present study, rats given ACR for three weeks had significantly lower total protein levels in their liver, kidney and testis, according to the results of the current study's histochemical protein identification analysis. ACR raised plasma phosphatases but dramatically reduced plasma protein levels and creatine kinase activity. In the liver and testis, transaminase and phosphatase activity were markedly reduced, while lactate dehydrogenase did not differ from the control group. Rats given ACR had higher levels of thiobarbituric acid reactive compounds as well as glutathione S-transferase and superoxide dismutase activities in their plasma, liver, testes, and kidney **(Yousef and El-Demerdash, 2006).** It has been shown that ACR and glycidamide may cause oxidative damage, immunological damage, and carcinogenicity in rat liver tissues at the histopathological, whole genome, and protein levels **(Chen *et al.*, 2018).** The testicular, hepatic, and renal tissues of the ACR + *M. oleifera* nanoparticles-treated group in this investigation were almost identical to those of the control group, with a few small variations still evident. Advantages might be brought about by its scavenging activity on free radicals, inhibition of lipid peroxidation processes, avoidance of free radical generation, and reduced levels of damage in these organs. The current results also demonstrated that administering ACR + *M. oleifera* nanoparticles to the rats for three weeks increased the amount of carbohydrates in the studied organs. Because *M. oleifera* leaves and seed extract are potent antioxidants that guard against the negative effects of free radical assault and oxidative

stress, this improvement was more noticeable in rats treated with ACR + *M. oleifera* nanoparticles than in rats treated with ACR alone**.**

Conclusion

ACR has adverse effects on rats; however, supplementing with *M. oleifera* nanoparticles could reduce these effects and assist the liver, kidney, and testis in returning to normal. It's possible that *M. oleifera's* anti-inflammatory and antioxidant properties account for its efficacy in mitigating pathological alterations brought on by ACR**.**

References

Abdel-Rahman, L. H., Al-Farhan, B. S., El-ezz, A., Sayed, A. E., Zikry, M. M., & Abu-Dief, A. M. (2022). Green Biogenic Synthesis of Silver Nanoparticles Using Aqueous Extract of Moringa Oleifera: Access to a Powerful Antimicrobial, Anticancer, Pesticidal and Catalytic Agents. Journal of Inorganic and Organometallic Polymers and Materials, 32(4):1422-1435.

Abduljalil, A. H. Y., Elbakry, K., Omar, N. A., Deef, L & Fahmy, S. (2023). Protective Effects of Silver Nanoparticles of Moringa Oleifera Leaves against Acrylamide-Induced Blood Toxicity in Rats. Scientific Journal for Damietta Faculty of Science, 12(2), 66-75.

Abduljalil, A. H. Y., Elbakry, K., Omar, N. A., Deef, L & Fahmy, S. (2024). Protective and Therapeutic Effects of Moringa oleifera Leave Nanoparticles against Acrylamide-Induced Hepato and Renal Toxicity in Adult Male Rats. Scientific Journal for Damietta Faculty of Science, 14(2), 1-12.

Aboulthana, W. M., Youssef, A. M., Seif, M. M., Osman, N. M., Sahu, R. K., Ismael, M., & Omar, N. I. (2021a). Comparative study between Croton tiglium seeds and Moringa oleifera leaves extracts, after incorporating silver nanoparticles, on murine brains. Egyptian Journal of Chemistry, 64(4):1709-1731.

Aboulthana, W. M., Shousha, W. G., Essawy, E. A. R., Saleh, M. H., & Salama, A. H. (2021b). Assessment of the Anti-Cancer Efficiency of Silver Moringa oleifera Leaves Nano-extract against Colon Cancer Induced Chemically in Rats. Asian Pacific Journal of Cancer Prevention: APJCP, 22(10): 3267.

Ahn, J. S., Castle, L., Clarke, D. B., Lloyd, A. S., Philo, M. R., & Speck, D. R. (2002). Verification of the findings of acrylamide in heated foods. Food Additives & Contaminants, 19(12):1116-1124.

Akinrinde, A. S., Oduwole, O., Akinrinmade, F. J., & Bolaji-Alabi, F. B. (2020). Nephroprotective effect of methanol extract of Moringa oleifera leaves on acute kidney injury induced by ischemia-reperfusion in rats. African health sciences, 20(3), 1382-1396.

Alkafafy, M. E., Sayed, S. M., El-Shehawi, A. M., El-Shazly, S., Farouk, S., Alotaibi, S. S., & Ahmed, M. M. (2021). Moringa oleifera ethanolic extract ameliorates the testicular dysfunction resulted from HFD-induced obesity rat model. Andrologia, 53(8), e14126.

Al Syaad, K. M., Al-Doaiss, A. A., Ahmed, A. E., El-Mekkawy, H., Abdelrahman, M., El-Mansi, A. A., & Ali, M. E. (2023). The abrogative effect of propolis on acrylamide-induced toxicity in male albino rats: Histological study. Open Chemistry, 21(1), 1–11.

Belhadj Benziane, A., Dilmi Bouras, A., Mezaini, A., Belhadri, A., & Benali, M. (2019). Effect of oral exposure to acrylamide on biochemical and hematologic parameters in Wistar rats. Drug and chemical toxicology, 42(2), 157-166.

Bhuiyan, M. E. J., Hossain, M. G., Saha, A., Islam, M. K., Bari, F. Y., Khan, M. A. H. N. A., & Akter, S. (2023). Protective roles of vitamin C and 5-aminosalicylic acid on reproduction in acrylamide intoxicated male mice. Saudi Journal of Biological Sciences, 30(8), 103738.

Chen, D., Liu, H., Wang, E., Yan, H., Ye, H., & Yuan, Y. (2018). Toxicogenomic evaluation of liver responses induced by acrylamide and glycidamide in male mouse liver. General physiology and biophysics, 37(2), 175-84.

Dharmendra, S., Vrat, A. P., Prakash, A. V., & Radhey, S. G. (2014). Evaluation of Antioxidant and Hepatoprotective Activities of Moringa oleifera Lam. Leaves in Carbon Tetrachloride-Intoxicated Rats. Antioxidants, 3, 569-591.

Drury RA, Wallington EA, & Cancerson R. (1976). Carlton's Histopathological Techniques, Oxford University Press, Oxford، UK, 4th edition.

Dobrzyńska, M. M. (2007). Assessment of DNA damage in multiple organs from mice exposed to X-rays or acrylamide or a combination of both using the comet assay. in vivo, 21(4), 657-662.

El-bakry, K., Toson, E. S., Serag, M., & Aboser, M. (2016). Hepatoprotective effect of Moringa oleifera leaves extract against carbon tetrachloride-induced liver damage in rats. World Journal of Pharmacy and Pharmaceutical Sciences, 5(5), 76-89.

El-Sharouny, S. H., El-Enein, R. A., ArsaniosSF, S. T. M., & Bayoumy, A. H. (2016). Acrylamide

induced liver toxicity and the possible protective role of vitamin E in adult male albino rat: histological, biochemical and histochemical study. The Egypt Journal of Medical Sciences, 37(2), 727-746.

Fahey, J. W. (2005). Moringa oleifera: a review of the medical evidence for its nutritional, therapeutic, and prophylactic properties. Part 1. Trees for life Journal, 1(5): 1-15.

Fiedan, I. O., Ahmed, E. A., & Omar, H. E. D. M. (2015). Acrylamide induced testicular toxicity in rats: protective effect of garlic oil. Biomarkers, 1(1), 5.

Gawesh, E. S., Hamdey, E. S., Abdelreheem Elshoura, A. I., & Abbas, M. A. (2021). Protective Effect of Cinnamon and Ginger on Acrylamide Induced Hepatotoxicity in Adult Male Albino Rats. International Journal of Medical Arts, 3(1), 1136-1144.

Ghorbel, I., Elwej, A., Fendri, N., Mnif, H., Jamoussi, K., Boudawara, T., & Zeghal, N. (2017). Olive oil abrogates acrylamide induced nephrotoxicity by modulating biochemical and histological changes in rats. Renal failure, 39(1), 236-245.

Gowda, S., Desai, P. B., Hull, V. V., Avinash, A. K., Vernekar, S. N., & Kulkarni, S. S. (2009). A review on laboratory liver function tests. The Pan african medical journal, 3.

Hamza, A. A. (2010). Ameliorative effects of Moringa oleifera Lam seed extract on liver fibrosis in rats. Food and Chemical Toxicology, 48(1), 345-355.

Jamshidi, K., & Zahedi, A. (2015). Acrylamide-induced acute nephrotoxicity in Rats. International Journal of Scientific Research in Science and Technology, 1(5):286-93.

Kadawathagedara, M., Botton, J., de Lauzon-Guillain, B., Meltzer, H. M., Alexander, J., Brantsaeter, A. L., & Papadopoulou, E. (2018). Dietary acrylamide intake during pregnancy and postnatal growth and obesity: Results from the Norwegian Mother and Child Cohort Study (MoBa). Environment international, (113): 325-334.

Kamalrudin, A., Jasamai, M., & Noor, M. M. (2018). Ameliorative effect of Moringa oleifera fruit extract on reproductive parameters in diabetic-induced male rats. Research Journal of Pharmacognosy,10, S54–S58.

Karimi, M. Y., Fatemi, I., Kalantari, H., Mombeini, M. A., Mehrzadi, S., & Goudarzi, M. (2020). Ellagic acid prevents oxidative stress, inflammation, and histopathological alterations in acrylamide-induced hepatotoxicity in wistar rats. Journal of dietary supplements, 17(6), 651-662.

Klaunig, J. E. (2008). Acrylamide carcinogenicity. Journal of agricultural and food chemistry, 56(15), 5984-5988.

Kandemir, F. M., Yıldırım, S., Kucukler, S., Caglayan, C., Darendelioğlu, E., & Dortbudak, M. B. (2020). Protective effects of morin against acrylamide-induced hepatotoxicity and nephrotoxicity: A multi-biomarker approach. Food and Chemical Toxicology, 138, 111190.

LoPachin, R. M., Barber, D. S., He, D., & Das, S. (2006). Acrylamide inhibits dopamine uptake in rat striatal synaptic vesicles. Toxicological Sciences, 89(1), 224-234.

Mahmood, K. T., Mugal, T., & Haq, I. U. (2010). Moringa oleifera: a natural gift-A review. Journal of Pharmaceutical Sciences and Research, 2(11): 775.

Mahmood, S. A., Amin, K. A., & Salih, S. F. (2015). Effect of acrylamide on liver and kidneys in albino wistar rats. International Journal of Current Microbiology and Applied Sciences, 4(5), 434-44.

Malathi, R., Chandrasekar, S., & Sivakumar, D. (2018). Assessment of toxicity study of ethanolic extract and synthesized silver nanoparticles of Moringa concanensis Nimmo leaves using wister albino rats. International Journal of Current Research in Life Sciences, 7(03):1250-1254.

Mazia, D., Brewer, P. A., & Alfert, M. (1953). The cytochemical staining and measurement of protein with mercuric bromphenol blue. The Biological Bulletin, 104(1), 57-67.

Nilanjuna, G., Samrat, P., & Piyali, B. (2014). Silver nanoparticles of Moringa oleifera–green synthesis, characterisation and its antimicrobial efficacy. Journal of Drug Delivery and Therapeutics, (11): 20-25.

Omeodu, S., & Uahomo, P. (2023). Anti-hyperglycemic and hepatoprotective properties of combined aqueous leaf extract of vernonia amygdalina and moringa oleifera in experimentally induced. International Journal of Recent Research in Life Sciences, 10 (1), 1-7.

Ozbek, E. (2012). Induction of oxidative stress in kidney. International journal of nephrology, 2012(1), 465897.

Pearse, A. G. E. (1985). Histochemistry, theoretical and applied. 4th, Vol. 2. Churchill LTD, London.

Prakash, D., Singh, B. N., & Upadhyay, G. (2007). Antioxidant and free radical scavenging activities of phenols from onion (Allium cepa). Food chemistry, 102(4):1389-1393.

Ramaswamy, M., Solaimuthu, C., & Duraikannu, S. (2019). Antiarthritic activity of synthesized silver nanoparticles from aqueous extract of Moringa concanensis Nimmo leaves against FCA induced rheumatic arthritis in rats. Journal of Drug Delivery and Therapeutics, 9(3): 66-75.

Rizk, M. Z., Abo-El-Matty, D. M., Aly, H. F., Abd-Alla, H. I., Saleh, S. M., Younis, E. A., & Haroun, A. A. (2018). Therapeutic activity of sour orange albedo extract and abundant flavanones loaded silica nanoparticles against acrylamide-induced hepatotoxicity. Toxicology reports, 5, 929-942.

Saleh, A. S. (2018). Evaluation of hepatorenal protective activity of Moringa oleifera on histological and biochemical parameters in cadmium intoxicated rats. Toxin Reviews, 10, 8–1.

Shipp, A., Lawrence, G., Gentry, R., McDonald, T., Bartow, H., Bounds, J., & Van Landingham, C. (2006). Acrylamide: review of toxicity data and dose-response analyses for cancer and noncancer effects. Critical reviews in toxicology, 36(6-7):481-608.

Sikder, K., Sinha, M., Das, N., Das, D., Datta, S., & Dey, S. (2013): Moringa oleifera Leaf extract prevents in vitro oxidative DNA damage. Asian Journal of Pharmaceutical and Clinical Research, 6(2), 157-161.

Sun, R., Chen, W., Cao, X., Guo, J., & Wang, J. (2020). Protective effect of curcumin on acrylamide-induced hepatic and renal impairment in rats: Involvement of CYP2E1. Natural Product Communications, 15(3), 1934578X20910548.

Tice, R. R., Agurell, E., Anderson, D., Burlinson, B., Hartmann, A., Kobayashi, H., & Sasaki, Y. F. (2000). Single cell gel/comet assay: guidelines for in vitro and in vivo genetic toxicology testing. Environmental and molecular mutagenesis, 35(3), 206-221.

Tornqvist, M. (2005). Acrylamide in food: the discovery and its implications. Advances in experimental medicine and biology, 561, 1.

Yousef, M. I., & El-Demerdash, F. M. (2006). Acrylamide-induced oxidative stress and biochemical perturbations in rats. Toxicology, 219(1-3), 133-141

الملخص العربي

عنوان البحث: الفحص النسيجي والكيمونسيجي للتأثيرات السامة للأكريلاميد والمحسن باستخدام الجسيمات النانووية لورق المورينجا أوليفيرا على كبد وكلى وخصية ذكور الجرذان البالغة

قدري البكري[١]، ناهد عمر[١]، لمياء ضيف[١]، شيرين فهمي[١]، عبدالله يعقوب[١]

[١] قسم علم الحيوان – كلية العلوم – جامعة دمياط.

تهدف الدراسة الحالية إلى تقييم تأثيرات إعطاء الجسيمات النانووية لأوراق المورينجا أوليفيرا والأكريلاميد على ذكور الجرذان البالغة . المورينجا أوليفيرا (M. oleifera) هي نبات ذو خصائص مضادة للأكسدة، في حين أن مادة الأكريلاميد (ACR) هي مادة كيميائية ضارة موجودة في الأطعمة منخفضة البروتين وعالية الكربوهيدرات. تم إنتاج جسيمات الفضة النانووية لأوراق المورينجا أوليفيرا وفحصها بإستخدام جهاز التحليل الطيفي للأشعة فوق البنفسجية والمرئية وجهاز تشتت الضوء الديناميكي والمجهر الإلكتروني النافذ. تم استخدام عشرين من ذكور الجرذان البالغة لمدة ثلاثة أسابيع، حيث قسمت عشوائياً إلى أربع مجموعات : مجموعة ١ : المجموعة الضابطة . مجموعة٢ :مجموعة الأكريلاميد، تم إعطائها الأكريلاميد (٥٠ مجم / كجم من وزن الجسم في مياه الشرب لمدة ثلاثة أسابيع) ؛مجموعة ٣: مجموعة جسيمات الفضة النانووية لأوراق المورينجا أوليفيرا (أعطيت الجرذان ٥٠ مجم / كجم من وزن الجسم عن طريق الفم). مجموعة٤ :مجموعة الأكريلاميد + جسيمات الفضة النانووية من المورينجا أوليفيرا (أعطيت الجرذان ٥٠مجم / كجم من وزن الجسم لكلاً منهما عن طريق الفم في نفس الوقت). تم جمع عينات الدم والأنسجة لإجراء الدراسات الفسيولوجية والنسيجية والكيمونسيجية عليها.

كشفت دراسة الأنسجة أن الجرذان التي تعرضت لمادة الأكريلاميد أصيبت بأضرار كبيرة في الكبد و الكلى والخصيتين، إلى جانب التغيرات الالتهابية والتشوهات الهيكلية. أدى العلاج باستخدام الجسيمات النانووية لأوراق المورينجا أوليفيرا إلى تحسين التغيرات النسيجية المرضية في الجرذان المصابة بالأكريلاميد، مما قلل من التعرض لسمية الأكريلاميد في مجموعة ذكور الجرذان البالغة المعالجة بالجسيمات النانووية لأوراق المورينجا أوليفيرا والأكريلاميد في نفس الوقت. استعادت الأسابيع الثلاثة من معالجة الجسيمات النانووية لأوراق المورينجا أوليفيرا إلى حد كبير الانخفاض الملحوظ كيمونسيجيا في البروتينات والكربوهيدرات. أدى استخدام الجسيمات النانووية لأوراق المورينجا أوليفيرا مع الأكريلاميد إلى تقليل الضرر الكيمونسيجي الذي يسببه الأكريلاميد بشكل كبير. قلل أيضًا العلاج بالجسيمات النانووية لأوراق المورينجا أوليفيرا من التأثير الضار لمادة الأكريلاميد على مستويات الألنين أمينو ترانسفيريز ((ALTوأسبارتيت أمينو ترانسفيريز ((ASTو بيروكسيد الدهون (مالونديالدهيد) ((MDAومستوى الكرياتينين واليوريا مع ارتفاع ملحوظ في زيادة نشاط إنزيم (.(SODويشير هذا إلى استخدام الجسيمات النانووية لأوراق المورينجا أوليفيرا كعامل وقائي للخلايا ضد السمية المرضية لمادة الأكريلاميد.